A Proposal of a Buoyancy Power Generator (tentative)

Yoji Ishihara
Maniwa, Okayama, JP
website: https://y-ishihara.info/
Mon., Nov. 15th, 2021

Abstract

A Buoyancy Power Generator (tentative; hereafter, BPG) is composed of a sealed container with water, two rotary disks with their positions fixed in the container, and some cages which are arranged in a loop at regular intervals on the wire. At the top and the bottom of this loop of cages, they turn along the rotary disks whose rotation is transmitted to the outside generator. Inside each cage, a watertight weight can move smoothly and divides it into two rooms; one is a vacuum, and the other is filled with water, where the water can go in and out freely through the water vents. Within a certain shallow depth, since the water pressure which pushes up the weight is smaller than the gravity on it, it touches the bottom of the cage on the upward side, and there is a vacuum above it. Consequently, cages on the upward side have larger buoyancy than those on the downward side. Firstly, a dynamic analysis is conducted for both downward and upward sides separately. Secondly, the driving force of a BPG is evaluated by adding up their resultant forces, and it is maximized in mathematical studies. They reveal the following three points. (1) The height and the area of the base of a cage and the density of a weight should be as large as possible. (2) The distance between adjoining cages should be as short as possible. (3) The height of a weight should account for $(\rho + \rho_0)/2\rho$ of that of a cage where ρ, ρ_0 are the densities of the weight, water respectively. Finally, quantitative simulations evaluate the driving force of each BPG with different shapes and dimensions of cages, namely (A) standard cages, (B) flat cages, and (C) slender cages. The results of them are as follows: (A) 39.2 (N), (B)117.6 (N), and (C) 196 (N).

1. Introduction

Modern civilization depends heavily on fossil fuel, which causes air pollution, global warming, and climate change. Meanwhile electricity is said to be environmentally friendly energy; however, even today its main energy sources are fossil fuel and nuclear power which destroy the environment including the ecology of human beings. In this paper, an idea of a Buoyancy Power Generator (BPG) is proposed. It uses only buoyancy to generate electricity continuously. After the explanation of the whole structure of a BPG and the structure of an individual cage, the variables of a cage are set which are essential for the dynamic analysis described later.

To begin with, the whole structure of a BPG is explained. Figure 1 shows a diagram of a BPG. The sealed container is almost filled with water, and a small vacuum is above the water. In the water, some cages which are attached to the wire are arranged in a loop at regular intervals like a vertical conveyor-belt-shaped Ferris wheel. At the top and the bottom of this vertical loop of cages, they turn along two rotary disks like a bicycle chain. Rotary disks are individually fixed to the sealed container; of course, they can spin and are attached to the outside generator (see Fig. 2). Consequently, at the top and the bottom of this vertical loop of cages, they turn themselves upside down. Incidentally, it is assumed that the rotary disks spin clockwise in Fig. 1.

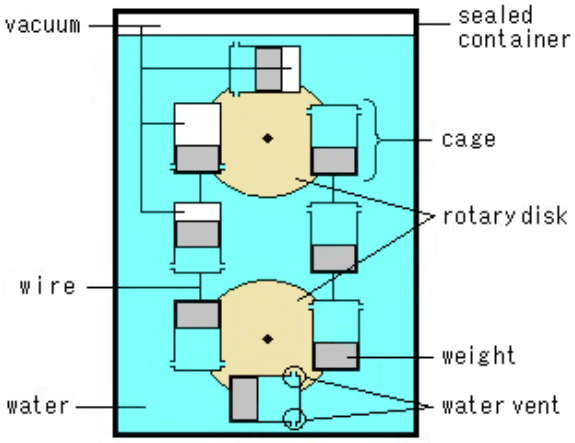

Figure 1. Diagram of BPG.

Figure 2 shows the upper part of a BPG seen obliquely from behind. The point is the mechanism which makes some difference in buoyancy between cages on the downward side and those on the upward side. It depends on the structure of an individual cage.

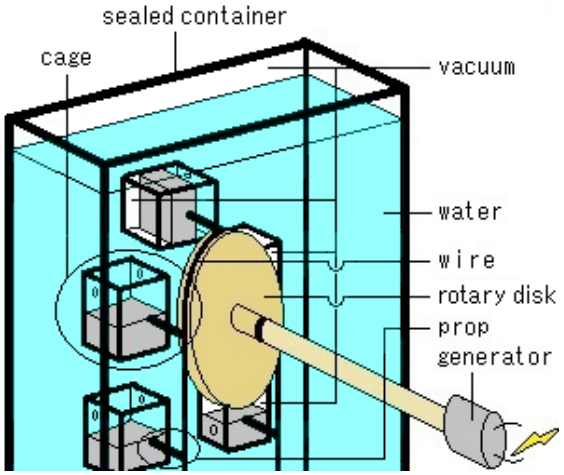

Figure 2. Upper part of BPG seen obliquely from behind.

The outer and the inner structure of an individual cage are shown in Fig. 3. Each cage is covered in a paper-thin outer frame, which is attached to the wire by a solid prop. Each prop doesn't bend nor twist. Each outer frame has two water vents on both sides of it. The water vents are located near the bottom of a cage on the upward side; naturally, they are located near the ceiling of a cage on the downward side.

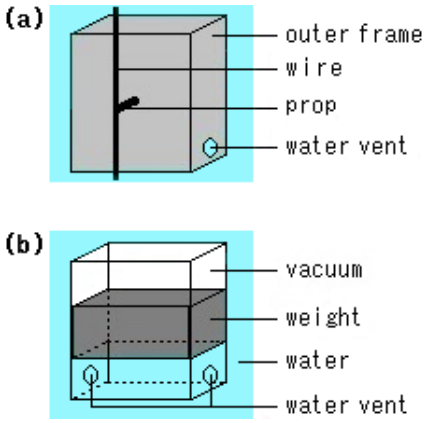

Figure 3. Structure of cage. **(a)** Outer structure. **(b)** Inner structure.

Inside each cage, there is a watertight weight which can move smoothly up and down. The weight divides the inside of the cage into two rooms; one is a vacuum, and the other is filled with water, where the water can go in and out freely through the water vents. Imaginably, the entrance and exit of the water are stopped when the water vents are obstructed by the weight. Within a certain shallow depth, on the upward side, the weight touches the bottom of the outer frame of the cage, because the water pressure which pushes up the weight is not as strong as the gravity on it. As a result, a vacuum is produced above the weight. This structure enables cages on the upward side to have larger buoyancy than those on the downward side in accordance with Archimedes' principle [1].

Before analyzing the forces, which act on a cage, the variables of a cage must be defined. They are shown in Fig. 4.

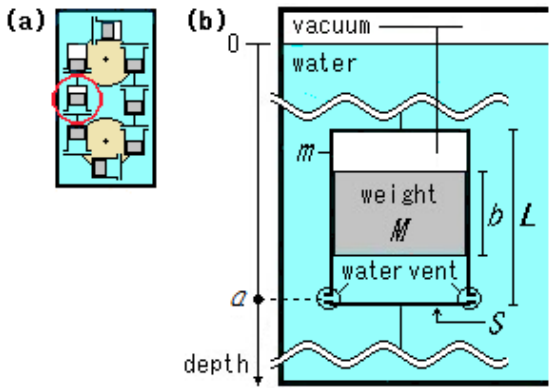

Figure 4. Definition of variables. **(a)** Overview of BPG in miniature; red circle denotes the position of the cage (the same applies hereafter). **(b)** Variables of cage.

First, Fig. 4(b) sets the axis of depth vertically downward; then, the origin is set at the boundary between the upper vacuum and the lower water inside the sealed container. In Fig. 4(b), a is the depth of the water vents of a cage on the upward side; S is the area of the base of a cage (it is a square) ; L is the height of a cage. b is the height of a weight; M is the mass of a weight; m is the mass of the outer frame of a cage. ρ is the density of the weight. These definitions of variables make it possible to analyze the forces which act on cages on the downward side and on the upward side separately.

2. Dynamic analysis on the downward side

The aim of this chapter is to analyze the forces which act on a cage (strictly, the outer frame of a cage; the same applies hereafter) on the downward side. A cage's 'going downward' described here is a hypothetical situation; however, it would be reasonable to analyze the forces which act on the outer frame of a cage, because this discussion doesn't take any forces into consideration that would derive from the cage's going downward itself. Additionally, only gravity and buoyancy on a cage are evaluated, then it is estimated that the outer frame of a cage transmits the resultant force of them to the wire. Ultimately, the driving force of a BPG is evaluated by adding up all these resultant forces on both the downward and upward sides. Figure 5 shows the forces which act on a cage on the downward side. On the downward side, the weight touches the bottom of the outer frame of a cage.

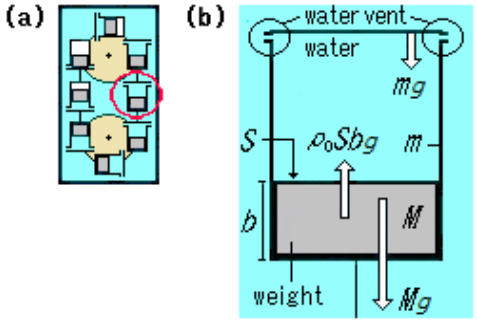

Figure 5. Gravity and buoyancy on downward side. **(a)** Overview of BPG in miniature. **(b)** Forces acting on cage.

Here, let the vertical downward direction be positive; the same applies hereafter. In Fig. 5(b), Mg and mg are gravity on the weight and on the outer frame of a cage respectively, and $\rho_0 Sbg$ is buoyancy. Then the resultant force F_d which acts on the outer frame of a cage is expressed as

$$F_d = (M+m)g - \rho_0 Sbg \ , \qquad (1)$$

where g is the acceleration of gravity, and the density of water is ρ_0; the same applies hereafter. Incidentally, the volume of the outer frame of a cage is so small that it can be ignored. As a result, F_d is a constant; it doesn't depend on the depth. To keep the cage at the same position, it must be held up with the equivalent force to F_d; hence, it can be estimated that the outer frame of a cage transmits the equivalent force to F_d to the wire if cages go at a constant speed.

Next, the analysis on the upward side is conducted.

3. Dynamic analysis on the upward side

The aim of this chapter is to analyze the forces which act on the outer frame of a cage on the upward side. As in the case of the previous chapter, a cage's 'going upward' described here is also a hypothetical situation; however, it would be reasonable to analyze the forces which act on the outer frame of a cage, because this discussion doesn't take any forces into consideration that would derive from the cage's going upward itself. The approach to the analysis is the same as that of the downward side; however, on the upward side, the cages must be classified into three groups by each depth of their water vents, because the resultant force which acts on the outer frame of a cage varies by the depth. It is the position of the weight in a cage that determines which group the cage belongs to. The three groups are as follows:

1. Weight touches the ceiling of the outer frame of a cage at an enough depth.
2. Weight doesn't touch the ceiling nor the bottom of the outer frame of a cage at a middle depth.
3. Weight lands on the bottom of the outer frame of a cage at a shallow depth.

To distinguish these three domains of depth of each cage's water vents, here two peculiar depths a_s and a_ℓ are defined (see Fig. 6(b)).

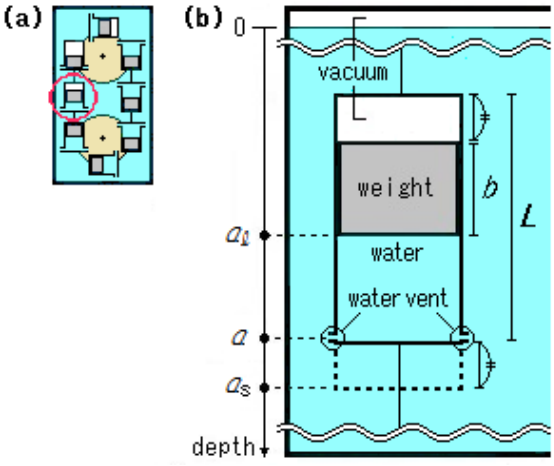

Figure 6. Positions of a_s and a_ℓ. **(a)** Overview of BPG in miniature. **(b)** Relationship between a_s and a_ℓ.

Firstly, it is about a_s. When a cage is in fully deep domain, the weight touches the ceiling of the outer frame of the cage because of the high water pressure. As the cage goes upward, the water pressure which pushes up the weight decreases linearly with respect to the depth. Soon the weight and the ceiling of the outer frame of the cage separate at a certain depth, which is defined as a_s. Strictly, a_s is the depth of the water vents of the cage when the weight and the ceiling of the outer frame of the cage separate; in fact, it is expressed as

$$a_s = \frac{M}{\rho_0 S} + L - b \ . \qquad (2)$$

Secondly, it is about a_ℓ. Once the weight and the ceiling of the outer frame of the cage separate, the weight remains at the same position, while the outer frame of the cage moves upward. Soon the weight lands on the bottom of the outer frame of the cage at a certain depth, which is defined as a_ℓ. Strictly, a_ℓ is the depth of the water vents of a cage when the weight lands on the bottom of the outer frame of the cage; in fact, it is expressed as

$$a_\ell = \frac{M}{\rho_0 S} \ . \qquad (3)$$

By using these a_s and a_ℓ, the three domains of depth described above can be expressed as follows:

1. $a_s < a$,
2. $a_\ell < a < a_s$,
3. $L < a < a_\ell$,

where a is the depth of the water vents of each cage on the upward side.

Next, a dynamic analysis on these three domains is conducted on the upward side.

3.1 Domain $a_s < a$

When the cage is in fully deep domain ($a_s < a$), the weight touches the ceiling of the outer frame of the cage as shown in Fig. 7.

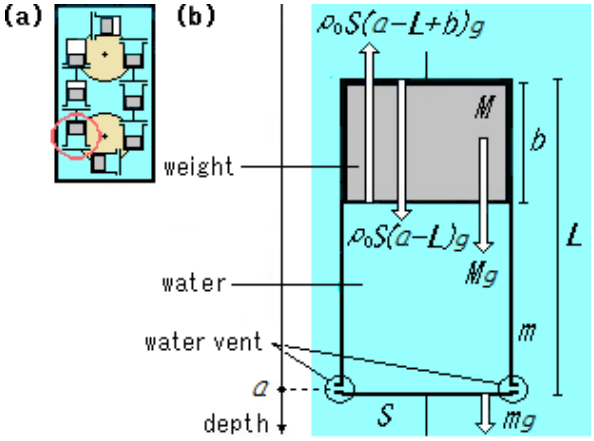

Figure 7. Gravity and water pressure on upward side when $a_s < a$. **(a)** Overview of BPG in miniature. **(b)** Forces acting on cage.

In one of the quantitative simulations, which are discussed later, the variables of each cage are set as follows: $S = 100$ (cm^2), $L = 20$ (cm), $b = 10$ (cm), $M = 11350$ (g), and $m = 50$ (g). A calculation shows that a_s=123.5 (cm). At deeper position than a_s, for example a=130 (cm), the water pressure pushes up the weight with 117.6 (N), while the gravity on the weight is 111.2 (N); hence, the weight would push up the ceiling of the outer frame of the cage with 6.4 (N) when the loop of cages are stationary. In Fig. 7(b), Mg and mg are gravity on the weight and on the outer frame of a cage respectively. The water pressure pushes the ceiling of the outer frame of the cage down with the force of $\rho_0 S(a-L)g$; it also pushes up the weight with the force of $\rho_0 S(a-L+b)g$. Therefore, the resultant force F_{u1} which acts on the outer frame of the cage is expressed as

$$F_{u1} = \rho_0 S(a-L)g + mg - \{\rho_0 S(a-L+b)g - Mg\} = (M+m)g - \rho_0 Sbg \ . \quad (4)$$

Thus, it turns out that $F_{u1} = F_d$. (See Eq. (1)). To keep the cage at the same position, it must be held up with the equivalent force to F_{u1}; hence, it can be estimated that the outer frame of a cage transmits the force F_{u1} to the wire if cages go at a constant speed.

3.2 Domain $a_\ell < a < a_s$

When the depth of the water vents of a cage is between a_ℓ and a_s ($a_\ell < a < a_s$), the outer frame of a cage goes upward; however, the weight remains at the same position as shown in Fig. 8(b).

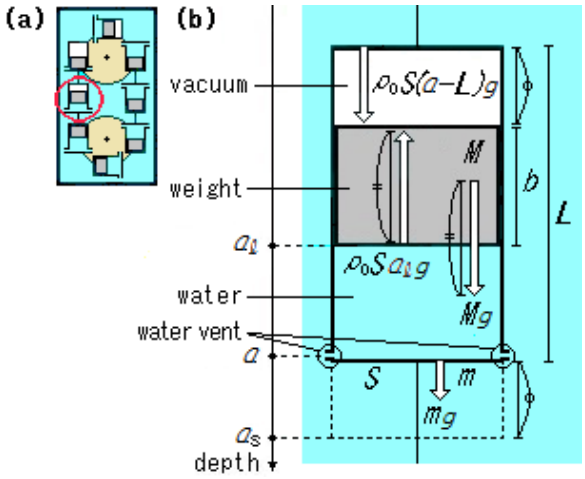

Figure 8. Gravity and water pressure on upward side when $a_\ell < a < a_s$. **(a)** Overview of BPG in miniature. **(b)** Forces acting on cage.

Here the weight doesn't affect the outer frame of a cage, because the weight can move smoothly inside the outer frame of a cage in accordance with the original assumption. The water pressure pushes the ceiling of the outer frame of a cage down with the force of $\rho_0 S(a-L)g$. Hence the resultant force F_{u2} which acts on the outer frame of a cage is expressed as

$$F_{u2} = \rho_0 S(a-L)g + mg \ . \quad (5)$$

Thus, in this domain of depth, the resultant force varies linearly depending on the depth of the water vents a. As in the case of the previous section 3.1, it can be estimated that the outer frame of a cage transmits the force F_{u2} to the wire.

3.3 Domain $L < a < a_\ell$

When the cage is within a certain shallow depth ($L < a < a_\ell$), the weight touches the bottom of the outer frame of a cage as shown in Fig. 9(b), because the water pressure which pushes up the weight is not as strong as gravity on it. Incidentally, the condition $L < a$ regulates the position of a cage not to be above the water surface (a=0) for the convenience of analysis. In Fig. 9(b), Mg and mg are gravity on the weight and on the outer frame of a cage respectively. The water pressure pushes the ceiling of the outer frame of a cage down with the force of $\rho_0 S(a-L)g$; it also pushes up the bottom of the outer frame of a cage with the force of $\rho_0 Sag$. Therefore, the resultant force

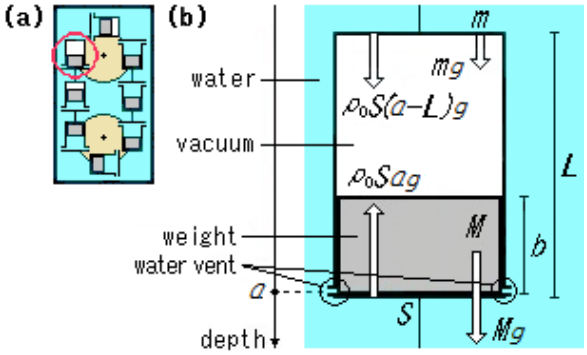

Figure 9. Gravity and water pressure on upward side when $L < a < a_\ell$. **(a)** Overview of BPG in miniature. **(b)** Forces acting on cage.

F_{u3} which acts on the outer frame of a cage is expressed as

$$F_{u3} = (M+m)g - \rho_0 SLg \ . \tag{6}$$

Thus, in this domain of depth, the resultant force F_{u3} is a constant; it doesn't depend on the depth. As in the cases of sections 3.1 and 3.2, it can be estimated that the outer frame of a cage transmits the force F_{u3} to the wire.

Next, it is necessary to combine the result of the analysis on the downward side with that on the upward side by applying two assumptions.

4. Two assumptions for combination of downward and upward sides

The aim of this chapter is to compare F_d with F_{u1}, with F_{u2}, and with F_{u3} in each domain of depth. Figure 10 schematically shows a diagram of a BPG; F_p represents the resultant force of a pair of cages on both the downward and the upward sides at the equal depth.

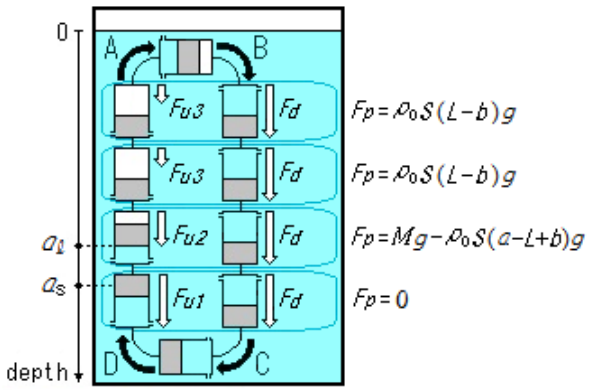

Figure 10. Resultant force F_p at each depth.

For the combination of the downward and the upward sides, the following two assumptions are practical.

Firstly, F_d is compared with F_{u1}, with F_{u2}, and with F_{u3}, and then the resultant force of them, namely F_p is calculated when the two cages of the downward and upward sides overlap accurately at the equal depth. Ultimately the driving force of the BPG is evaluated by adding up F_ps. Of course, cages don't move discontinuously like a second hand of a watch; however, a cage will meet the next cage of opposite side by moving about only half a cage. Therefore, this method for evaluation is not invalid.

Secondly, another assumption is made about four parts of the loop of cages where cages draw arcs A, B, C, and D in Fig. 10. It is possible to locate a rising cage on A (and on D) and a falling cage on C (and on B) in point symmetry by adjusting the cages' interval and the radius of the rotary disk. It can be assumed that the rising on A and on D are offset by the falling on C and on B respectively. Here is a concern that the falling on B might not be able to offset the rising on D effectively, because the water might not rush into the cage instantaneously at the start on B, namely the top of the loop of cages. However, it would not be a serious problem, for qualitatively the falling of the heavy cage on C more than makes up for the rising of the light cage on A; in fact, a certain capacity inside the cage is a vacuum all through A.

Then the resultant force F_p in each domain of depth is calculated by Eq. (7) where let the rotary disk's clockwise spin be positive.

$$F_p = F_d - F_{un} \ . \tag{7}$$
$$(n = 1, 2, 3)$$

Here, a is the depth of the water vents of a cage on the upward side.

4.1 F_p in the domain $a_s < a$

When the two cages of downward and upward sides overlap accurately with their bottoms located in fully deep domain ($a_s < a$), F_d and F_{u1} act on the outer frames of the cages on the downward and upward sides respectively. Therefore, the resultant force F_p is expressed as

$$F_p = F_d - F_{u1} = 0 \ , \tag{8}$$

where Eqs. (1) and (4) were substituted into Eq. (7). Consequently, no force is generated in this domain (see Fig. 10).

4.2 F_p in the domain $a_\ell < a < a_s$

When the two cages of downward and upward sides overlap accurately with their bottoms located between a_ℓ and a_s ($a_\ell < a < a_s$), F_d and F_{u2} act on the outer frames of the cages on

the downward and upward sides respectively. Here the resultant force F_p is expressed as

$$\begin{aligned} F_p &= F_d - F_{u2} \\ &= Mg - \rho_0 S(a - L + b)g \ , \end{aligned} \tag{9}$$

where Eqs. (1) and (5) were substituted into Eq. (7). As a consequence, the resultant force F_p varies linearly depending on the depth of the water vents of a cage on the upward side (see Fig. 10). Obviously at most one pair of cages which overlap accurately can exist in this domain of depth.

4.3 F_p in the domain $L < a < a_\ell$

When the two cages of downward and upward sides overlap accurately with their bottoms located within a certain shallow depth ($L < a < a_\ell$), F_d and F_{u3} act on the outer frames of the cages on the downward and upward sides respectively. Hence, the resultant force F_p is expressed as

$$\begin{aligned} F_p &= F_d - F_{u3} \\ &= \rho_0 S(L - b)g \ , \end{aligned} \tag{10}$$

where Eqs. (1) and (6) were substituted into Eq. (7). Thus, the resultant force F_p is a constant in this domain of depth (see Fig. 10). In contrast to the previous section, more than one pairs of cages, which overlap accurately, can exist in this domain of depth. Naturally, the more pairs of cages exist in this domain, the more powerful driving force the BPG has.

Figure 11 schematically shows the results of sections 4.1, 4.2, and 4.3; on the graph, the horizontal axis represents the depth of the water vents of a cage on the upward side, and the vertical axis represents the resultant force F_p.

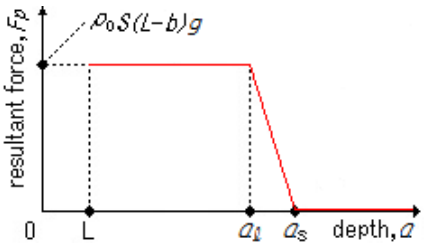

Figure 11. Relationship between F_p and a.

Next, it must be considered how to maximize the driving force of a BPG.

5. Maximization of the driving force of BPG

In the previous chapter, F_ps were calculated in each domain of depth. No force was generated in the domain $a_s < a$. In the domain $a_\ell < a < a_s$, at most one pair of cages could exist, and F_p depended on the depth a complexly. Therefore, from now on, these two domains ($a_s < a$, and $a_\ell < a < a_s$) are excluded from the evaluation of the driving force of a BPG; consequently, the attention is focussed only on the domain $L < a < a_\ell$. This method for evaluation doesn't overestimate the actual value, because it omits the domain $a_\ell < a < a_s$ which can contribute a little to the driving force of a BPG. For example of Fig. 10, two F_ps of the highest and the second highest pairs of cages are added up to evaluate the driving force of a BPG. Accordingly, it is necessary to grasp how many pairs of cages can exist in this domain $L < a < a_\ell$.

For these needs, three parameters α, β, and γ should be introduced here. They represents the occupation rate of the weight to the cage, the ratio of the distance between adjoining cages to L, and the ratio of the width of the cage to L respectively.

Figure 12 schematically shows α, β, and γ, where cages on the downward side are omitted for the sake of simplicity. Let d be the distance between adjoining cages when they are merely rising or falling, and let ℓ be one side of the square base of a cage. Parameters α, β, and γ are expressed as follows:

$$b = \alpha L \ , \tag{11}$$

$$d = \beta L \ , \tag{12}$$

$$\ell = \gamma L \ . \tag{13}$$

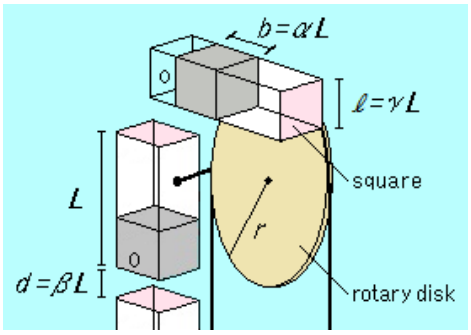

Figure 12. Diagram of parameters α,β, and γ.

Incidentally, r represents the radius of the rotary disk. Using these parameters makes it possible to find some conditions to maximize the driving force of a BPG, which is represented as P here. Since $(a_\ell - L)/(L + d)$ pairs of cages exist in the domain $L < a < a_\ell$, P is calculated by

$$P = \rho_0 S(L - b)g \times \frac{a_\ell - L}{L + d} \ . \tag{14}$$

Here substitution of Eqs. (3), (11), (12), and $M = \rho S b$ (ρ is the density of the weight) into Eq. (14), and then completing the square leads to the following equation.

$$P = -\frac{1}{1+\beta} SLg\rho \left\{ (\alpha - \frac{\rho + \rho_0}{2\rho})^2 - \frac{\rho^2 - 2\rho_0\rho + \rho_0^2}{4\rho^2} \right\} \ . \tag{15}$$

Consequently, when $\alpha = (\rho + \rho_0)/2\rho$, P reaches a local maximum P_{max} which is expressed as

$$P_{max} = \frac{1}{1+\beta} SLg \frac{\rho^2 - 2\rho_0\rho + \rho_0^2}{4\rho} \ . \qquad (16)$$

Thus, S, L, and ρ should be as large as possible; meanwhile, β should be as small as possible. Furthermore, the height of a weight b should account for $(\rho + \rho_0)/2\rho$ of the height of a cage L; in fact, quantitative simulations discussed later adopt $\alpha = 0.5$, for the sake of simplicity. Incidentally, they adopt $\rho = 11.35(\mathrm{g/cm^3})$; it is lead [2]. Here the theoretically ideal value is $\alpha = 0.54$.

Next, a geometrical study minimizes β by using the relationship between β and γ.

6. Minimization of β

In this chapter, a mathematical analysis reveals the conditions for cages' turning smoothly around rotary disks without a collision between any adjoining cages, and aims to minimize β under such conditions. To begin with, the radius of the rotary disk r is set so that cages are arranged at an angle of every $\pi/2$ (rad) around the center of the upper rotary disk as shown in Fig. 13. The size of the lower rotary disk is the same as this.

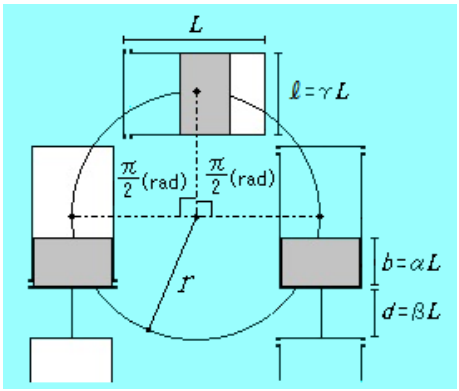

Figure 13. Arrangement of cages around upper rotary disk.

Here, r is calculated by

$$r = \frac{2(L+d)}{\pi} \ . \qquad (17)$$

Obviously r is regulated by the next condition

$$r > \frac{1}{2}(L + \ell) \ . \qquad (18)$$

Substitution of Eqs. (12), (13) and (17) into this inequality (18) leads to the following inequality

$$\beta > \frac{\pi}{4}\gamma + \frac{\pi - 4}{4} \ . \qquad (19)$$

Figure 14 geometrically shows adjoining cages around the upper rotary disk. The circle is the upper rotary disk. At the moment when the cage changes its movement from vertical rising to turning, its rotation angle θ is set $\theta = 0$. C_1' and C_2' are centers of the adjoining cages; when θ was null, C_1', C_2' were at C_1, C_2 respectively. Here the domain of θ is restricted to $0 < \theta < \pi/2$, because in the domain $\pi/2 < \theta < \pi$, relative positions of the adjoining cages don't change; in fact, they only turn from positions at 12 and 9 o'clock to positions at 3 and 12 o'clock respectively. In Fig. 14, a line segment P_1P_2 is the shortest distance between the adjoining cages. Accordingly, the aim is to find the minimum of β which satisfies the condition $0 < P_1P_2$ and inequality (19) for any θ on $0 < \theta < \pi/2$. By using variables and parameters β and γ, the condition $0 < P_1P_2$ is expressed as

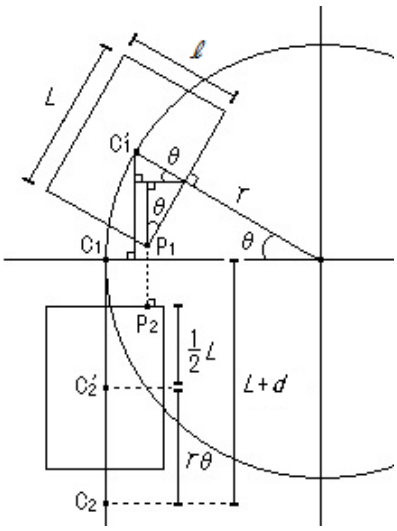

Figure 14. Adjoining cages around upper rotary disk.

$$P_1P_2 = r\sin\theta - \frac{1}{2}(\ell\sin\theta + L\cos\theta) + (L+d) - \frac{1}{2}L - r\theta > 0 \ . \qquad (20)$$

Substitution of Eqs. (12), (13), and (17) into this inequality (20) leads to the following inequality

$$\beta > \frac{2\theta - \frac{\pi}{2} + \frac{\pi}{2}\cos\theta + (\frac{\pi}{2}\gamma - 2)\sin\theta}{2\sin\theta + \pi - 2\theta} \ . \qquad (21)$$

Let the right side of this inequality (21) be $f(\theta)$, namely

$$f(\theta) = \frac{2\theta - \frac{\pi}{2} + \frac{\pi}{2}\cos\theta + (\frac{\pi}{2}\gamma - 2)\sin\theta}{2\sin\theta + \pi - 2\theta} \ . \qquad (22)$$

Figure 15(a) shows the results of plotting $f(\theta)$ against θ for three different γs as follows: (A) γ=0.5, (B) γ=1, and (C) γ=0.125. These (A), (B), and (C) represent standard cages, flat cages, and slender cages respectively; in fact, three quantitative simulations with these cages are conducted in the next chapter. Figure 15(b) is the partially magnified graph around the local maximum of (C) in Fig. 15(a).

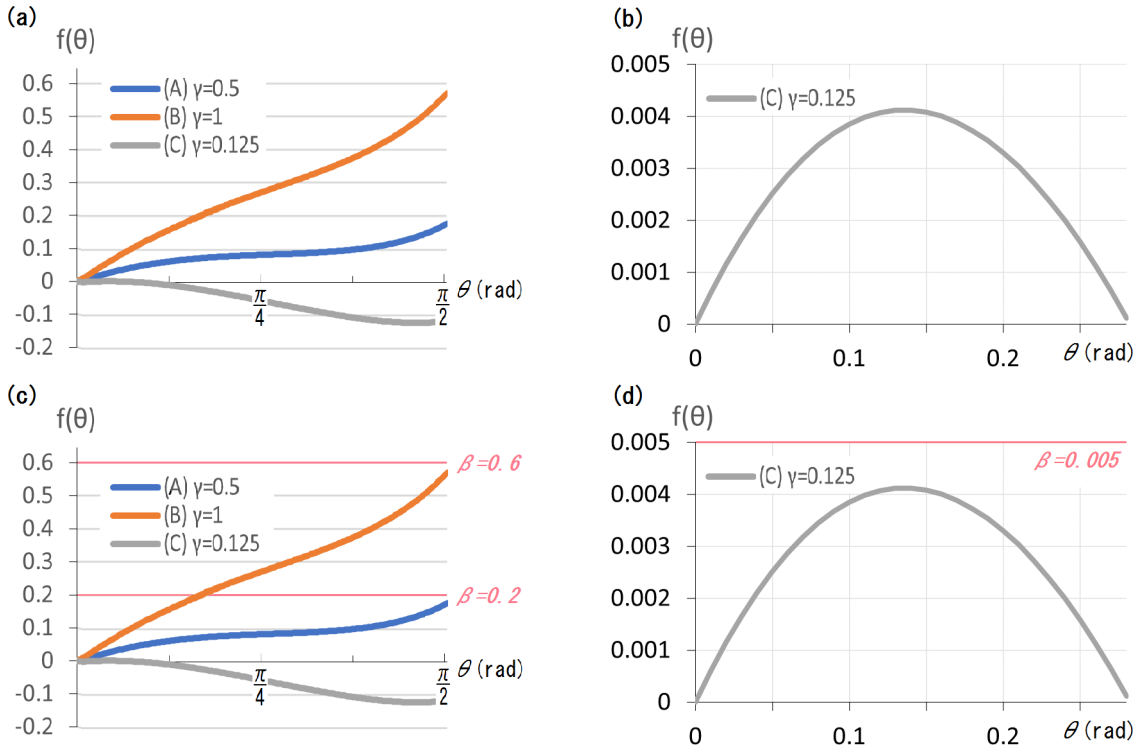

Figure 15. Changes in $f(\theta)$ and fixed β in each simulation. **(a)** $f(\theta)$ plotted against θ for three different γs in each simulation. **(b)** Magnified graph of (C) in **(a)** around its local maximum. **(c)** Each β fixed for simulations (A) and (B). **(d)** Magnified graph of (C) in **(c)** around its local maximum and β fixed for simulation (C) in the same way as simulations (A) and (B).

In each case, β can be fixed so that it slightly exceeds the maximum of $f(\theta)$ on $0 < \theta < \pi/2$; in fact, βs are fixed as follows: (A) $\beta = 0.2$, (B) $\beta = 0.6$, and (C) $\beta = 0.005$, as shown in Fig. 15(c) and 15(d). Incidentally, each of these βs satisfies the inequality (19).

Next, quantitative simulations are conducted on three cases with these βs and γs.

7. Quantitative evaluation of driving force of BPG by simulation

In this chapter, the driving force of each BPG is evaluated in each simulation for the following three different shapes and dimensions of cages: (A) standard cages ($\gamma = 0.5$), (B) flat cages ($\gamma = 1$), and (C) slender cages ($\gamma = 0.125$), which match the analysis of the previous chapter. Table 1 shows values of all variables and parameters which are used in each simulation (A), (B), and (C).

Table 1. Dimensions, mass, and all parameters of a cage for each simulation.
n: simulation label; S: area of the base of a cage; L: height of a cage; ℓ: width of a cage;
b: height of a weight; M: mass of a weight; m: mass of the outer frame of a cage;
ρ_0: density of water; ρ: density of a weight; α: ratio of b to L; β: ratio of d to L; γ: ratio of ℓ to L;
d: distance between adjoining cages; r: radius of rotary disks.

n	S (cm^2)	L (cm)	ℓ (cm)	b (cm)	M (g)	m (g)	ρ_0 (g/cm^3)	ρ (g/cm^3)	α	β	γ	d (cm)	r (cm)
(A) standard	100	20	10	10	11 350	50	1 (water)	11.35 (lead)	0.5	0.2	0.5	4	15.28
(B) flat	400	20	20	10	45 400	50	1	11.35	0.5	0.6	1	12	20.37
(C) slender	100	80	10	40	45 400	50	1	11.35	0.5	0.005	0.125	0.4	51.18

7.1 Simulation (A) standard cages

The BPG with standard cages for simulation (A) is designed in Fig. 16.

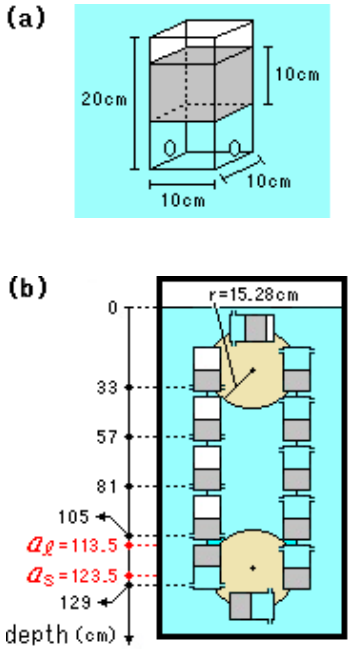

Figure 16. Design for BPG with standard cages for simulation (A). **(a)** Dimensions of standard cage. **(b)** Schematic diagram of BPG.

By setting r appropriately, it is possible to arrange three cages at 9, 12, and 3 o'clock along the upper rotary disk and another three cages at 3, 6, and 9 o'clock along the lower rotary disk simultaneously in line symmetry as shown in Fig.16(b). In fact, r and d are set r = 15.28 (cm), and d = 4 (cm) here. The driving force of the BPG is evaluated by adding up F_ps at the moment when both of the cages (downward and upward sides) overlap accurately at the equal depth, which occurs every time they move just only half (strictly, $(L+d)/2$) a cage; the same applies hereafter. Simple calculations show a_s= 123.5 (cm), and a_ℓ= 113.5 (cm) (see Eqs. (2) and (3)). Referring to Fig. 16(b), F_ps of the top four pairs of cages are added up to evaluate the driving force of the BPG. That is

$$\rho_0 S(L-b)g \times 4 = 39.2 \ \ (\mathrm{N}) \ . \qquad (23)$$

Consequently, although it may have small oscillation in strength, this BPG is estimated to have a driving force of 39.2 (N) continuously. Incidentally, this oscillation would be caused by cages' falling and rising along the arcs of rotary disks; the same applies also in simulations (B) and (C).

7.2 Simulation (B) flat cages

Next, the BPG with flat cages for simulation (B) is designed in Fig. 17.

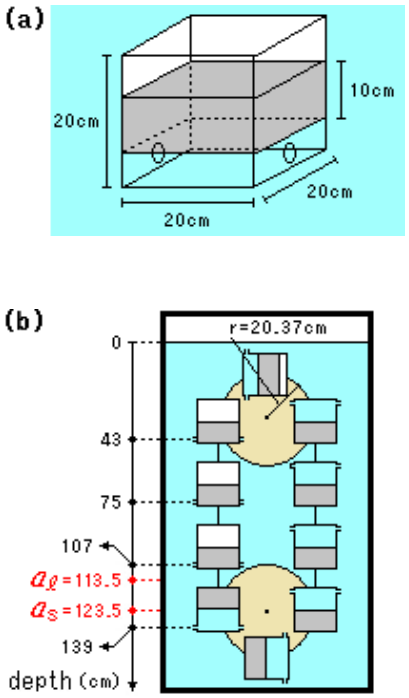

Figure 17. Design for BPG with flat cages for simulation (B). **(a)** Dimensions of flat cage. **(b)** Schematic diagram of BPG.

In simulation (B), the area of the base of a cage S is four times as large as that in simulation (A) as shown in Fig. 17(a). Here r and d are set r = 20.37 (cm), and d = 12 (cm), so that all cages are located in line symmetry in the same way as simulation (A) (see Fig. 17(b)). In simulation (B), the cages' distance d is much longer than that in simulation (A). That is because cages in simulation (B) are much flatter than those in simulation (A). Simple calculations show a_s = 123.5 (cm), and a_ℓ = 113.5 (cm), which are the same as they are in simulation (A) (see Eqs. (2) and (3)). Referring to Fig. 17(b), F_ps of the top three pairs of cages are added up to evaluate the driving force of the BPG. That is

$$\rho_0 S(L-b)g \times 3 = 117.6 \ \ (\mathrm{N}) \ . \qquad (24)$$

In simulation (B), the number of pairs of cages which contribute to the driving force of the BPG is smaller than that in simulation (A). That is because the cages' distance d in simulation (B) is longer than that in simulation (A). As a result, it is estimated that this BPG continuously has a driving force of 117.6 (N), which is three times as large as that in simulation (A).

7.3 Simulation (C) slender cages

Finally, the BPG with slender cages for simulation (C) is designed in Fig. 18.

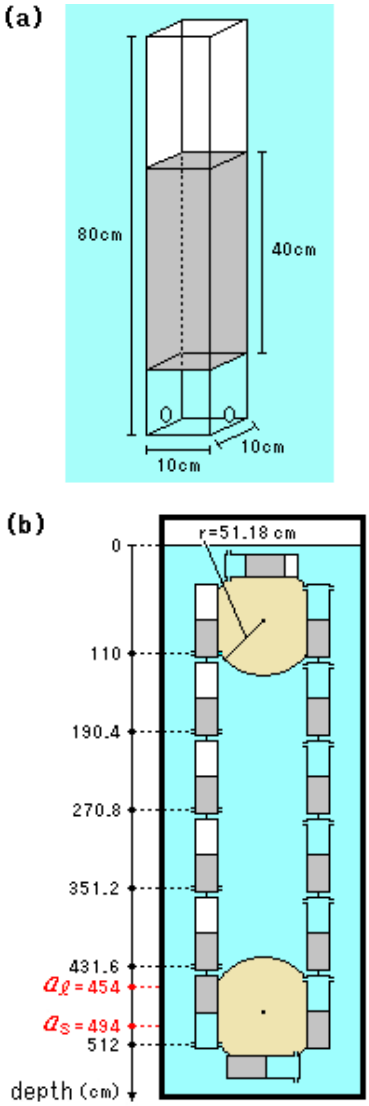

Figure 18. Design for BPG with slender cages for simulation (C). **(a)** Dimensions of slender cage. **(b)** Schematic diagram of BPG.

In simulation (C), the height of a cage and a weight (L and b) are four times as high as that in simulation (A) as shown in Fig. 18(a). Here r and d are set $r = 51.18$ (cm), and $d = 0.4$ (cm), so that all cages are located in line symmetry in the same way as simulations (A) and (B) (see Fig. 18(b)). In simulation (C), the cages' distance d is much shorter than that in simulation (A). That is because β in simulation (C) is far smaller than that in simulation (A), which is due to a remarkable reduction in γ. Simple calculations show a_s = 494 (cm), and a_ℓ = 454 (cm) (see Eqs. (2) and (3)). Referring to Fig. 18(b), F_ps of the top five pairs of cages are added up to evaluate the driving force of the BPG. That is

$$\rho_0 S(L-b)g \times 5 = 196 \ \text{(N)} \ . \qquad (25)$$

In simulation (C), the number of pairs of cages which contribute to the driving force of the BPG is larger than that in simulation (A). That is because the cages' distance d in simulation (C) is shorter than that in simulation (A). As a consequence, it is estimated that this BPG continuously has a driving force of 196 (N), which is five times as large as that in simulation (A).

8. Conclusion

In this paper, the idea of a Buoyancy Power Generator (BPG) has been proposed. It continuously generates electricity only by buoyancy. In its structure, cages have been designed so that different forces in strength act when turned upside down. This structure has enabled cages on the upward side to have larger buoyancy than those on the downward side. With respect to the maximization of the driving force of a BPG, theoretically the following three points have been revealed. (1) The height and the area of the base of a cage, and the density of the weight in a cage should be as large as possible. (2) The distance between adjoining cages should be as short as possible. (3) The ratio of the height of a weight to the height of a cage should be $(\rho+\rho_0)/2\rho$ where ρ and ρ_0 are the densities of a weight and water respectively. In fact, three quantitative simulations have evaluated the driving force of each BPG with different shapes and dimensions of cages, namely (A) standard cages, (B) flat cages, and (C) slender cages. Finally, the results have been obtained as follows: (A) 39.2 (N), (B) 117.6 (N), and (C) 196 (N), which confirms the theory described above. An issue to be resolved is the inner structure of a cage which enables the weight to move smoothly inside it keeping one end of it to be a vacuum.

Acknowledgments

Despite the historical, social, and legal nature of this kind of paper, a few advisors offered the author constructive suggestions. A thousand thanks for their continuous interest, and also deepest gratitude to everyone who would read through this paper.

References

[1] Archimedes, "On Floating Bodies," in T. L. Heath (ed.), *The works of Archimedes* (DOVER PUBLICATIONS, INC., Mineola, New York, 2002), pp.253-262.

[2] Health & Chemicals Department, *Profiles of the Initial Environmental Risk Assessment of Chemicals*, Vol. 8, No.1-II-(III)-[3], p.2, Ministry of the Environment, March 2010. http://www.env.go.jp/chemi/report/h22-01/pdf/chpt1/1-2-3-03.pdf